Chapter 3

Effective Internal Impedance

Conductor loss calculation constitutes a major part of lossy transmission line analysis. High-speed digital interconnects can be considered as transmission lines. Knowledge of the loss on the interconnect would lead to better and faster design. As a performance limiting factor, the loss would set the maximum interconnect length and degrade signal quality. The conductor loss can also be used as an attenuation mechanism to remove unwanted signals from the interconnect.

When solving for conductor loss, the representation of conductors are important. Several techniques exist to include finite conductivity in two dimensional field analysis. In this chapter, an **e**ffective **i**nternal **i**mpedance (EII) approach will be explained to represent conductors in a transmission line structure. The conformal mapping technique, used extensively to solve for two dimensional structures with perfect conductors is modified to include conductor loss through the EII approach. The filament technique can profit in computation time and problem size using the EII approach.

The effective internal impedance of a conductor can be viewed as a quantity to represent the volume of the conductor on the surface of the conductor in terms of resistance and energy stored inside. In calculation of EII, each

conductor is considered isolated in space. Through an external solver, then they are permitted to interact. Hence, EII is not the surface impedance with other conductors present. With other conductors, the field distribution would change and the surface impedance would differ from that of an isolated conductor.

3.1 Surface Impedance

On a surface of a conductor, the ratio of the tangential electric field to the tangential magnetic field is a constant at a given frequency and is called *surface impedance*. S. A. Schelkunoff, in 1934 described surface impedance for use in coaxial cable calculations [32]. Schelkunoff solved the wave equations assuming small disturbances to TEM fields with finite conductivity materials for coaxial structures. Experimental work has been done to verify the concept [29]. The surface impedance of a semi-infinite metal can be calculated assuming plane wave incidence. The surface impedance for this case is the driving point impedance seen by the incident wave at the surface of the metal, which is given by

$$Z_s = \sqrt{\frac{j\omega\mu}{\sigma}}, \tag{3.1}$$

where ω is the frequency in radians per second, and μ and σ are the permittivity and conductivity in the metal, respectively. This result is also very accurate when the wave is incident at an oblique angle. It can be proved using Snell's law that refracted wave in the metal propagates close to normal even for a large angle of incidence. The angle of refraction for 90° incidence angle is given by

$$\theta_2 = \sin^{-1}\sqrt{\frac{\omega\epsilon}{\sigma}}. \tag{3.2}$$

From the equation above we can deduce that for frequencies lower than $\sigma/2\pi\epsilon$[1] the refracted angle is very close to 0°. For $\epsilon = 8.85 \times 10^{-12} F/m$ and $\sigma = 5.8 \times 10^7 1/(\Omega\text{m})$, $\sigma/2\pi\epsilon = 6.554 \times 10^{18}$Hz.

Using the surface impedance concept in electromagnetic analysis is not new. The boundary element formulation removes conductors from the domain by means of the surface impedance concept. A finite element method approach utilized surface impedance to reduce the problem size and the computation time [8]. Most common way of treating surface impedance is valid at high frequency when the field penetration is smaller than the thickness of the conductors.

In this chapter, a way of representing the internal behavior of conductors using an effective internal impedance concept from dc to high frequencies will be explained. As mentioned before, the concentration will be on the calculation of an isolated conductor surface impedance.

3.1.1 Surface Impedance Near Sharp Edges

Electromagnetic problems with finite conductivity metals are usually large in terms of computer resources due to abruptly changing fields near conductor boundaries. Using an impedance boundary condition (IBC), the problem can be reduced to an exterior one for which the solution can be simplified. Equation (3.1) is widely used as the impedance boundary condition. This approach assumes the ratio of tangential electric field to tangential magnetic field is constant. Near sharp edges, due to the interaction from the other face, this assumption is not valid. As the penetration depth decreases compared to the conductor size, the error introduced also decreases due to the fact that to be able to see

[1] $\sigma/2\pi\epsilon$ is also called the dielectric relaxation frequency.

the effect of the other face, we need to be "closer" to the corner. While this assumption is valid at high frequencies, solutions to some low frequency problems suffer a considerable amount of error. A modified impedance boundary condition has been proposed by W. Jingguo and J. D. Lavers to model low frequency behavior more accurately [21]. In the modified impedance boundary condition, plane waves (Transverse Magnetic) incident normal to the faces are assumed. Inside the conductor, the total field is obtained as the sum of refracted plane waves at the faces. For an infinite wedge of conductor with an angle α the surface impedance along one side, is given by

$$Z_s = \sqrt{\frac{j\omega\mu}{\sigma}} \frac{1 + e^{-\beta x \sin\alpha}}{1 - e^{-\beta x \sin\alpha} \cos\alpha}, \tag{3.3}$$

where ω is the frequency in rad/s. This result is obtained assuming the incident plane waves are of the same magnitude. Equation (3.3) is accurate enough to study the behavior of surface impedance at high frequencies in the vicinity of a corner.

Figure (3.1) illustrates the frequency behavior of surface impedance with respect to the distance from the corner for a 90° angle. The surface impedance is normalized to the characteristic wave impedance in the conductor, e.i., $\sqrt{j\omega\mu/\sigma}$. The dotted line in Fig. 3.1 is the skin depth ($\delta = \sqrt{2/\omega\mu\sigma}$) plotted against frequency. The corner is *visible* in the vicinity of about 3δ. The surface impedance takes the form of the characteristic impedance of the conductor when the corner is more than 3δ away. The modified surface impedance concept can be used to calculate surface impedance of an isolated rectangular conductor. In the next section this approach will be applied to rectangular conductors together with other ways of approximating surface impedance.

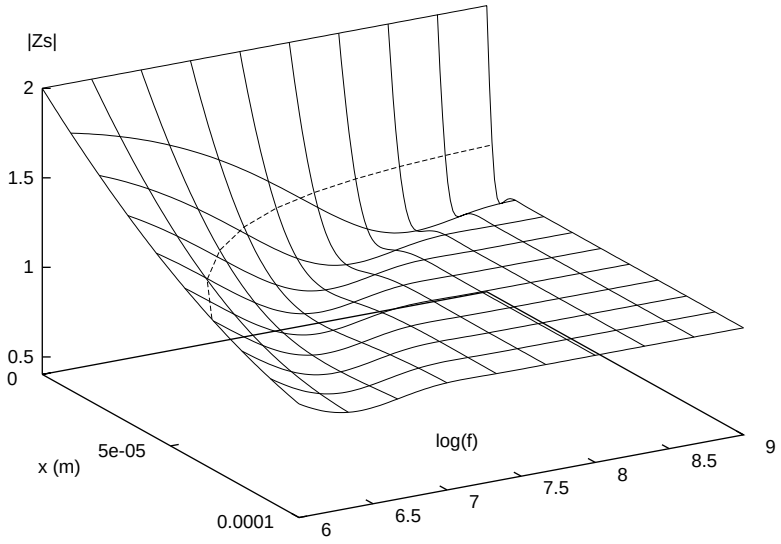

Figure 3.1: Normalized surface impedance (see text) versus distance (x) from the corner in meters and logarithm of frequency (in Hz) with $\alpha = \pi/2$ in (3.3). The dotted line is the skin depth versus frequency.

3.2 Effective Internal Impedance of Rectangular Cylindrical Conductors

Conductors with rectangular cross-section constitute a major part of interconnect structures used in today's high-speed digital circuits. With faster rise times and higher clock rates, the conductor loss in the interconnect structures becomes important. As design parameters are getting tighter, designers need tools to calculate transmission line characteristics of an interconnect structure more efficiently and accurately. The characteristics of digital signals require a model to be valid for a wide bandwidth, from dc to frequencies on the order of the inverse of the rise time. As will be explained in the proceeding chapters, de-coupling the electromagnetic behavior into one of external and one of internal to the conductors proves to be an efficient and accurate technique to solve such problems. The internal characteristics of each conductor are calculated by finding the effective internal impedance of the conductor in the absence of all other conductors.

The method of calculating the effective internal impedance is not unique, although the techniques used should work at dc as well as at high frequencies. This would provide a simple and efficient model for the effective internal impedance concept. In the following section headings, the letter labels the technique for later reference.

3.2.1 A. Modified Surface Impedance as EII

Jingguo et. al. [21] proposed a technique to calculate the surface impedance near a corner in the medium to high frequency range. In this section the application of this technique to rectangular conductors will be explained.

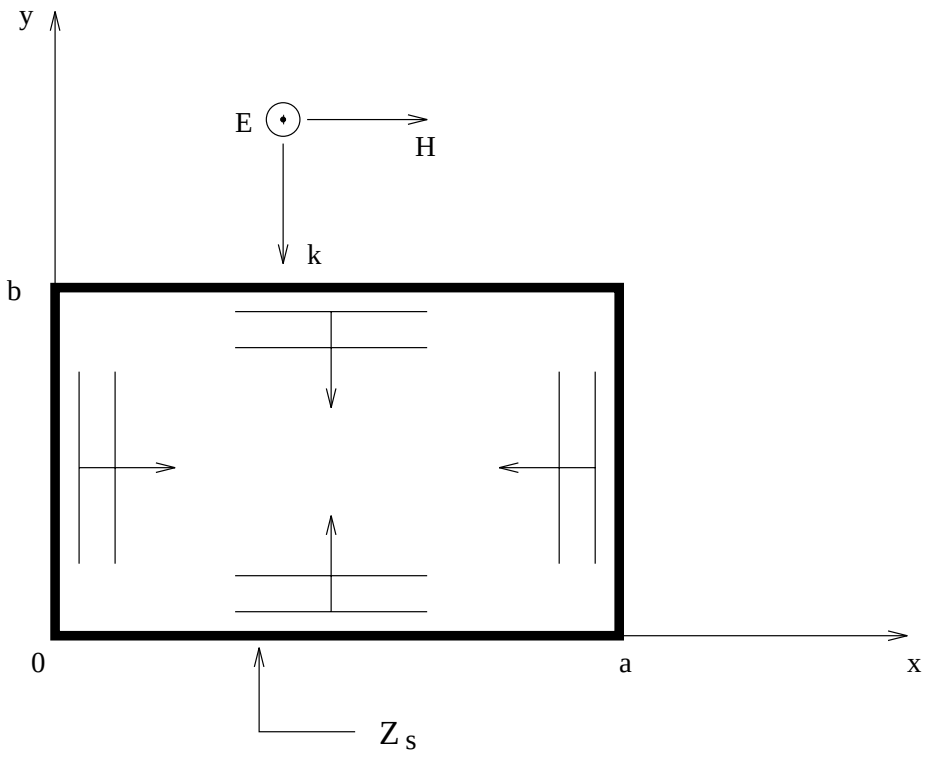

Figure 3.2: Calculation of surface impedance for a rectangular bar assuming plane wave propagation in the conductor from all surfaces. Calculated surface impedance is a function of frequency and location.

For a given rectangular conductor with width a and thickness b (Fig. 3.2), assuming uniform plane wave (TM) incident on all the four surfaces, the total magnetic field can be written inside the conductor as

$$\vec{\mathbf{H}} = H_0 \left[\left(\mathbf{e}^{-y\gamma} - \mathbf{e}^{(y-b)\gamma} \right) \hat{a}_x + \left(-\mathbf{e}^{-x\gamma} + \mathbf{e}^{(x-a)\gamma} \right) \hat{a}_y \right], \tag{3.4}$$

where γ is the complex propagation constant in the conductor and H_0 is the magnitude of the magnetic field. Using $\nabla \times \vec{\mathbf{H}} = \sigma \vec{\mathbf{E}}$, the electric field inside the conductor can be calculated as

$$\vec{\mathbf{E}} = H_0 \sqrt{\frac{j\omega\mu}{\sigma}} \left(\mathbf{e}^{-x\gamma} + \mathbf{e}^{(x-a)\gamma} + \mathbf{e}^{-y\gamma} + \mathbf{e}^{(y-b)\gamma} \right) \hat{a}_z. \tag{3.5}$$

The ratio of tangential electric field to the tangential magnetic field at the surface will yield to the surface impedance at that point,

$$Z_s(x, y = 0) = \frac{E_z}{H_x} = \sqrt{\frac{j\omega\mu}{\sigma}} \frac{\mathbf{e}^{-x\gamma} + \mathbf{e}^{(x-a)\gamma} + 1 + \mathbf{e}^{-b\gamma}}{1 - \mathbf{e}^{-b\gamma}}. \tag{3.6}$$

Equation (3.6) is a simple and convenient approximation to the actual surface impedance. At low frequency, the dc resistance of the conductor should be obtained using (3.6). Taking the limit as $\omega \to 0$, the surface impedance at the top and bottom surfaces reduces to

$$Z_s(x, y = 0)|_{dc} = \frac{4}{\sigma b}. \tag{3.7}$$

Similarly, the surface impedance at dc can be obtained for the left and right hand side surfaces as $4/\sigma a$. Since Z_s is constant over the surface that it is valid on, the total resistance introduced by that surface is the ratio of surface impedance to the width of the surface. Again, notice that the geometries under consideration are two dimensional. Hence, the total dc resistance can be calculated by the

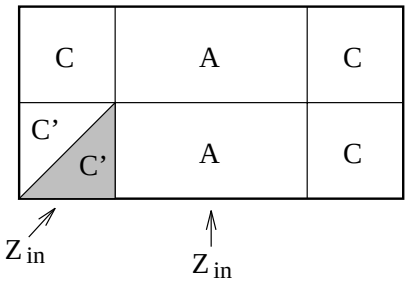

Figure 3.3: Segmentation of rectangular bar into sections of four squares and two rectangles. For rectangular sections (3.9) is used. to calculate EII

parallel sum of individual surfaces,

$$R_{dc} = \left[\left(\frac{2}{\sigma b}\frac{1}{a}\right)^{-1} + \left(\frac{2}{\sigma a}\frac{1}{b}\right)^{-1}\right]^{-1} = \frac{1}{\sigma ab}. \tag{3.8}$$

At high frequency, where the skin-depth is less than both dimensions of the conductor, (3.6) reduces to (3.3) near the corners and to $\sqrt{j\omega\mu/\sigma}$ in the middle.

3.2.2 B. Geometrical Segmentation

Assuming the thickness of the conductor is much smaller than the width, the surface impedance can be calculated using

$$Z_{eii} = \frac{\sqrt{j\omega\mu/\sigma}}{\tanh(\sqrt{j\omega\mu\sigma}\frac{t}{2})}, \tag{3.9}$$

where t is the thickness of the conductor. As the thickness becomes comparable to the width, (3.9) can not capture the surface impedance behavior of the conductor. A simple approach is to divide the conductor into segments as in Fig. 3.3 and calculate the driving point impedance at the base for each section separately. The rectangular sections will have EII given by (3.9). By symmetry, obtaining the EII as a function of position for half of the square region

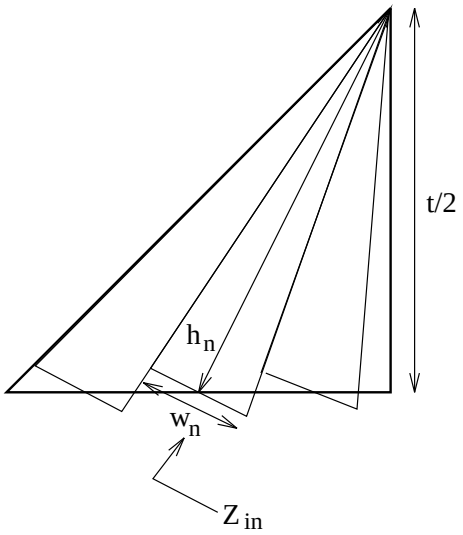

Figure 3.4: Each right triangular corner section is further divided into isocelase triangles, and input impedance at the base is calculated to obtain EII for corresponding section on the surface.

(C'), divided along a diagonal is sufficient. To capture this effect, the triangular corner half piece is divided into N triangular patches (Fig. 3.4). Then the height of each triangle is used as the "thickness" of this segment of conductor, hence mimicking a wave propagating from the base of the triangle to the apex, through a nonuniform transmission line. For the nth ($n = 0, 1, 2, ..., N-1$) segment, the height h_n is given by

$$h_n = \frac{t}{2}\sqrt{1 + \left(\frac{n+0.5}{N}\right)^2} \tag{3.10}$$

and the width w_n (Fig. 3.4) by

$$w_n = \frac{h_n}{2}\left[\frac{1}{N + (n+0.5)\frac{n}{N}} + \frac{1}{N + (n+0.5)\frac{n+1}{N}}\right]. \tag{3.11}$$

For a triangular section, the surface impedance expression can be found by applying transverse resonance and non-uniform transmission line analysis [38, 28]. The total input impedance for a triangular transmission line with

width w_n at the input end, plate separation of unit distance and length h_n, filled with a uniform conducting material of conductivity σ is multiplied with the width projected to the surface of the conductor (i.e., $t/2N$) to obtain the EII of the nth section,

$$Z_{eii}^{n} = \frac{j\sqrt{j\omega\mu\sigma}}{w_n\sigma}\frac{\mathbf{J}_0(j\sqrt{j\omega\mu\sigma}h_n)}{\mathbf{J}_1(j\sqrt{j\omega\mu\sigma}h_n)}\frac{t}{2N}, \tag{3.12}$$

where $\mathbf{J}_0$ and $\mathbf{J}_1$ are Bessel functions of the first kind. The position-dependent EII in the corner region is thus represented by N position-independent EIIs, one for each $t/2N$ width of the surface.

At low frequency, (3.12) reduces to the dc resistance of the triangular section. At high frequency, by redistribution of current to the base of the triangles, the impedance of each section is given by

$$Z_{eii} = \frac{1}{w_n}\sqrt{\frac{j\omega\mu}{\sigma}} \tag{3.13}$$

instead of

$$Z_{eii} = \frac{2N}{t}\sqrt{\frac{j\omega\mu}{\sigma}} \tag{3.14}$$

except in the vicinity of corners.

3.2.3 C. Modified Geometrical Segmentation

Investigation of (3.6) reveals that at high enough frequencies the corner of the conductor is visible within a 3δ (where δ is the skin depth in the conductor) distance. The EII for points away from the corner more than 3δ is equal to (3.1). Observing this fact, the geometrical segmentation technique explained in the previous section can be modified to increase accuracy and efficiency in calculation. The depth the calculation is conducted in the conductor is set to

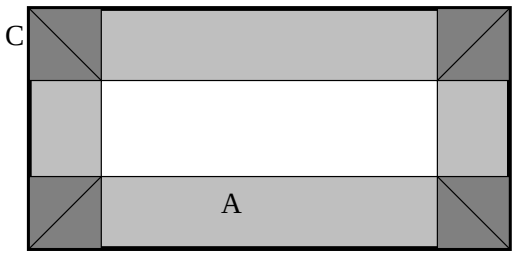

Figure 3.5: Calculation of effective internal impedance for a rectangular bar by keeping only 3δ thick metal from the surface. Because of skin-effect, at 3δ into the metal the fields are negligible.

3δ. This is achieved by making the conductor a hollow tube, with wall thickness of 3δ as the frequency increases (Fig. 3.5). For the central rectangular regions, 'A' (3.9) is used with $t/2 = 3\delta$ and for corner sections, 'C' similar geometrical segmentation applied as in section 3.2.2. However, since the thickness of the wall is always 3δ the argument to the special functions (hyperbolic tangents and the Bessel functions in (3.9) and (3.12)) is always the same once the frequency is high enough such that 3δ is smaller than the thickness of the conductor. For lower frequencies the dc resistance is used for that section.

3.2.4 D. Alternative Geometrical Segmentation Technique

To calculate the effective internal impedance, the cross section of the conductor is divided into two triangles on the narrower sides and two trapezoids on the wider sides. As discussed in the previous sections this is the basic segmentation to capture wave behavior inside the conductor. Further segmentation is necessary to increase accuracy.

As a final example of an EII, the calculation can be done by first segmenting the conductor into two triangles and two trapezoids as described above. For each segment the hyperbolic tangent expression, (3.9) is used with $t/2$ as a

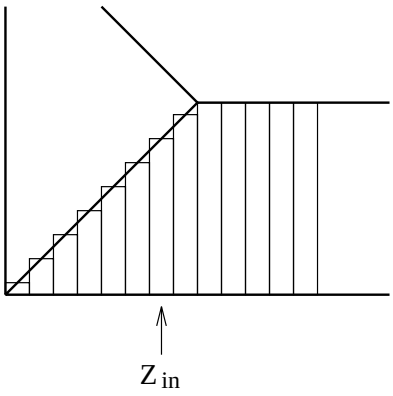

Figure 3.6: Alternate geometrical segmentation for calculating EII, subdividing each section further into rectangular pieces.

function of position on surface such that $t/2$ is equal to the depth of the segment at that location (Fig. 3.6). Although the dc resistance is accurate, the corner pieces at high frequencies does not capture correct frequency dependence. The resistance of a segment in the corner region is proportional to one over the distance between the segment and the corner. As a result the corner segments have a sharp increase in resistance, even at dc. This pushes the dc current distribution away from the corner. The hard discontinuity introduced by this method does not allow current to crowd to corners even at high frequencies.

3.3 Comparison of Effective Internal Impedance Calculation Techniques

We can investigate the accuracy of the techniques introduced above at low and high frequency. At low frequency, the current is uniform over the cross section of the conductor. As the frequency increases the current starts to crowd towards edges and surface due to internal proximity and skin effects. The techniques proposed above need to account for these effects accurately.

At low frequency, the required parameter is dc resistance. All the techniques give the dc resistance accurately. Another parameter to check at low frequency is internal inductance which represents energy stored in the volume of the conductor. This parameter is important to obtain an accurate low to high frequency transition for frequency dependent inductance and resistance. Internal inductance is calculated for various aspect ratio rectangular conductor bars as the difference of total inductance to external inductance. The total inductance is calculated using an analytic expression [39]. The external inductance is calculated using the Ribbon Method (Chapter 5). The current is distributed using ribbons on the surface such that $\hat{n} \times \vec{H}$ is equal to the surface current density. This forces magnetic field inside to diminish (from the Surface Equivalence Theorem [4]). Hence inductance calculated using the surface currents will result in the external inductance. The internal inductance from the effective internal impedance techniques is calculated using the stored energy equation,

$$L_{int} = \lim_{\omega \to 0} \frac{\oint |J_s|^2 \Im \{Z_{eii}\} \, d\ell}{\omega \left| \oint J_s d\ell \right|^2} \tag{3.15}$$

where J_s is the current distribution on the surface determined by the real part of Z_{eii} at dc and $\Im$ denotes the imaginary part. Figure 3.7 illustrates the comparison between internal inductance calculation and the various effective internal impedance calculations for different aspect ratios. It should be noted that internal inductance does not depend on the size of the conductor, but the aspect ratio. For an aspect ratio of one (i.e., a square), the results are very close to the more rigorous result. As the aspect ratio increases, the conductor becomes a thin plate, and the internal effective impedance for techniques B, C, and D is simply given by (3.9). For an aspect ratio equal to 100, the difference

between techniques B, C, and D and the internal inductance is 3.77nH/m. For a 1m by 1cm conductor strip, the total low frequency inductance is 0.3μH/m. Hence approximating the internal behavior using techniques B, C, and D results in 1.25% error for a 1m wide strip. For the purposes of this work the total inductance of geometries under consideration is much bigger than the example presented above. For PCB wire connections and MCM interconnect structures the error is not significant.

Results from technique A increases as the aspect ratio increases contrary to the internal inductance calculated using the filament technique and surface equivalent current approach. From the derivation of technique A it can be concluded that it does not include the reflecting fields at the surfaces to account for the stored energy inside the conductor.

At high frequency, when the field penetration is small compared to the cross sectional size of the conductor, estimating internal behavior on the surface is also physically a good approximation. A quantity to compare effective internal impedance to is the actual surface impedance at frequencies where the field penetration is smaller than the thickness of the conductor. Figure 3.8 compares he surface impedance calculated using the filament technique with effective internal impedances calculated using techniques explained above for a rectangular copper bar at 5GHz. All the techniques approximates the surface impedance well. Techniques A and C are particularly very close to the actual surface impedance.

The effective internal impedance approximates internal behavior of the conductor on the surface from dc to high frequency. All the methods proposed herein would get the crucial parameters, series resistance at dc, and frequency

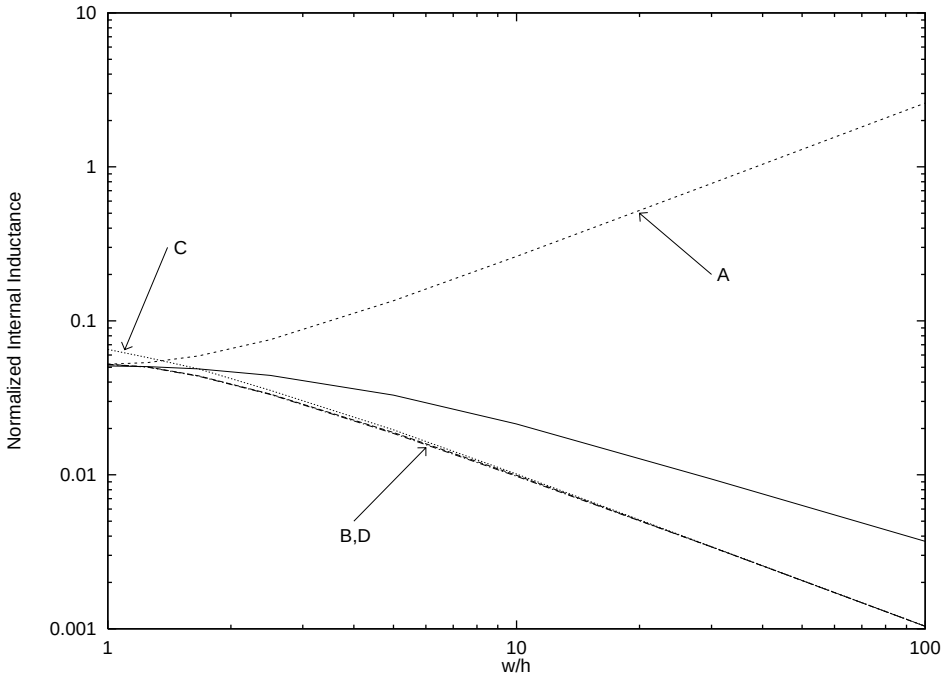

Figure 3.7: Internal inductance normalized to μ versus aspect ratio for a single conductor at dc. Solid curve is calculated from ribbon technique and surface equivalent current calculation, curve A is from the modified surface impedance concept, curve B and C are from geometrical segmentation and modified version of it, respectively, curve D is from the alternate technique.

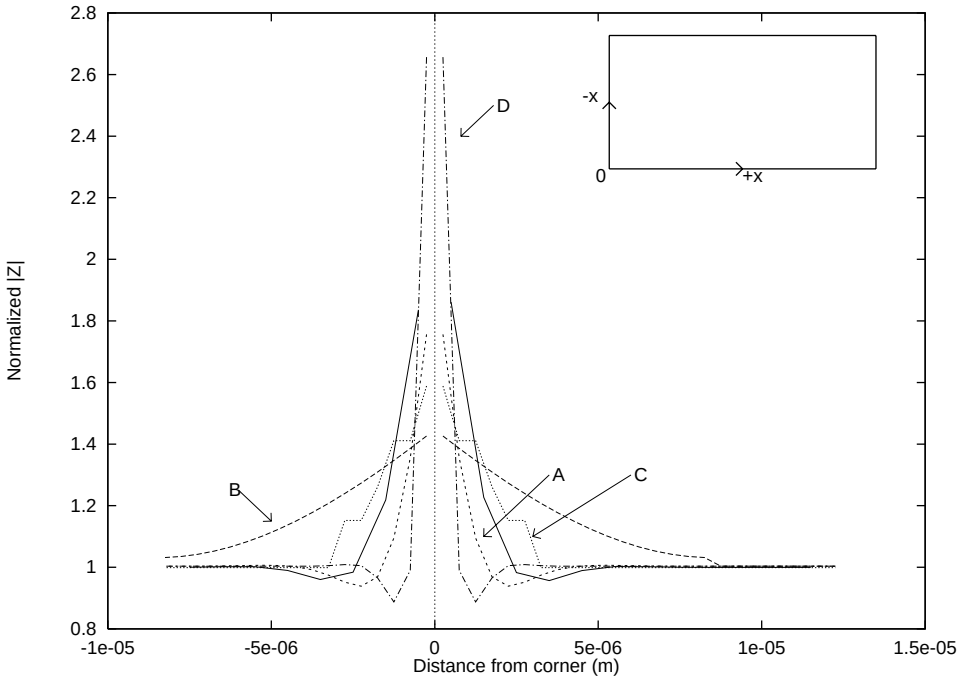

Figure 3.8: Comparison of magnitude of EII and surface impedance versus distance from the corner of a 25μm wide, 17μm thick rectangular copper bar. Solid line is the surface impedance calculated using filament technique.

dependent resistance and internal inductance at higher frequencies, with reasonable accuracy. The next step is to use this approach in an external solver to obtain total frequency dependent series impedance values for a given transmission line structure. In the following chapters two external field solving schemes are explained, the conformal mapping and the ribbon techniques.